Ultraviolet and ionizing radiation enhance the growth of BCCs and trichoblastomas in patched heterozygous knockout mice

MICHELLE ASZTERBAUM[1], JOHN EPSTEIN[1], ANTHONY ORO[2], VANJA DOUGLAS[1], PHILIP E. LEBOIT[3], MATTHEW P. SCOTT[4] & ERVIN H. EPSTEIN JR.[1]

[1]*Department of Dermatology, University of California San Francisco, Building 100, Room 269, 1001 Potrero Ave, San Francisco, California 94110, USA*

[2]*Department of Dermatology, Stanford University, P210, 1201 Welch Road, Stanford, California 94305, USA*

[3]*Department of Dermatology and Pathology, University of California San Francisco 1701 Divisadero Ave, San Francisco, California 94115, USA*

[4]*Departments of Developmental Biology and Genetics and Howard Hughes Medical Institute, 279 Campus Drive, Stanford University School of Medicine, Stanford California A 94305, USA*

Correspondence should be addressed to E.H.E.; email: ehepstein@orca.ucsf.edu and M.P.S.; email: scott@cmgm.stanford.edu

Basal cell carcinomas, the commonest human skin cancers, consistently have abnormalities of the hedgehog signaling pathway and often have *PTCH* gene mutations. We report here that *Ptch*$^{+/-}$ mice develop primordial follicular neoplasms resembling human trichoblastomas, and that exposure to ultraviolet radiation or ionizing radiation results in an increase in the number and size of these tumors and a shift in their histologic features so that they more closely resemble human basal cell carcinoma. The mouse basal cell carcinomas and trichoblastoma-like tumors resemble human basal cell carcinomas in their loss of normal hemidesmosomal components, presence of *p53* mutations, frequent loss of the normal remaining *Ptch* allele, and activation of hedgehog target gene transcription. The *Ptch* mutant mice provide the first mouse model, to our knowledge, of ultraviolet and ionizing radiation-induced basal cell carcinoma-like tumors, and also demonstrate that *Ptch* inactivation and hedgehog target gene activation are essential for basal cell carcinoma tumorigenesis.

Basal cell carcinoma (BCC) is the commonest human cancer, affecting 750,000 Americans per year. Based on rapidly rising tumor incidence rates, it is estimated that almost one in three Caucasians born in the United States after 1994 will develop a BCC in their lifetime[1]. As with other skin cancers, BCC risk is correlated with degree of skin pigmentation and with exposure to ultraviolet radiation (UV) or ionizing radiation (IR). Patients affected by the rare autosomal dominantly inherited disorder known as the basal cell nevus syndrome (BCNS) have a substantially increased susceptibility to BCC (developing tens to hundreds of BCCs) and to extracutaneous tumors (medulloblastomas and rhabdomyosarcomas). Patients with BCNS inherit a defective copy of the tumor supressor gene *PTCH* (refs. 2,3). *PTCH* mutations and loss of the remaining wild-type allele have also been identified in sporadic basal cell carcinomas, trichoepitheliomas (a BCC-like tumor) and medulloblastomas, indicating a common genetic basis for the sporadic and syndrome-associated cancers[2,3,4,5,6].

The Ptch protein is a receptor for the diffusable hedgehog protein, is expressed in hedgehog target tissues in the developing mouse and fly and is an important regulator of embryonic pattern formation. The Ptch protein represses hedgehog target gene expression through its interaction with smoothened (Smoh), and this repression is relieved when Sonic hedgehog (Shh) binds to Ptch, or after mutational inactivation of Ptch. Smoh signaling may activate transcription of hedgehog targets, including *Ptch*, through activation of the putative transcription factor Gli. Therefore, mutational inactivation of *Ptch* and consequent loss of Ptch protein function results in increased *Ptch* expression and the accumulation of high levels of *Ptch* and *Gli* transcripts. *In situ* hybridization studies detect high levels of *PTCH* and *GLI1* message in almost all human BCCs, in contrast to the absence of message in normal epidermal keratinocytes, indicating that hedgehog pathway target gene activation is common to all human BCCs (refs. 7–10).

Murine models of cutaneous carcinogenesis induced by ultraviolet irradiation have yielded an expanded understanding of the genetic and cellular events of squamous cell carcinoma (SCC) tumorigenesis. In contrast, study of BCC tumorigenesis has been hampered by the an inexplicable failure of mutagenic chemicals, UV or IR to induce BCCs in mice[11]. BCC-like tumors have been described in the skin of mice (*Shh* and mutant *Smoh* transgenic mice) and frog embryos (*Gli1*-transfected) with epidermal hedgehog pathway activation[9,12,13]. However, the transgenic mice either can not reproduce (*Smoh*^{mut} transgenic) or fail to survive the perinatal period (*Shh* transgenic). *Ptch* heterozygote knockout mice (exons 1/2 or 6/7 deleted) have multiple BCNS-associated developmental abnormalities, including jaw cysts and polydactyly, and also a high incidence of tumors, including medulloblastomas and rhabdomyosarcomas, but have

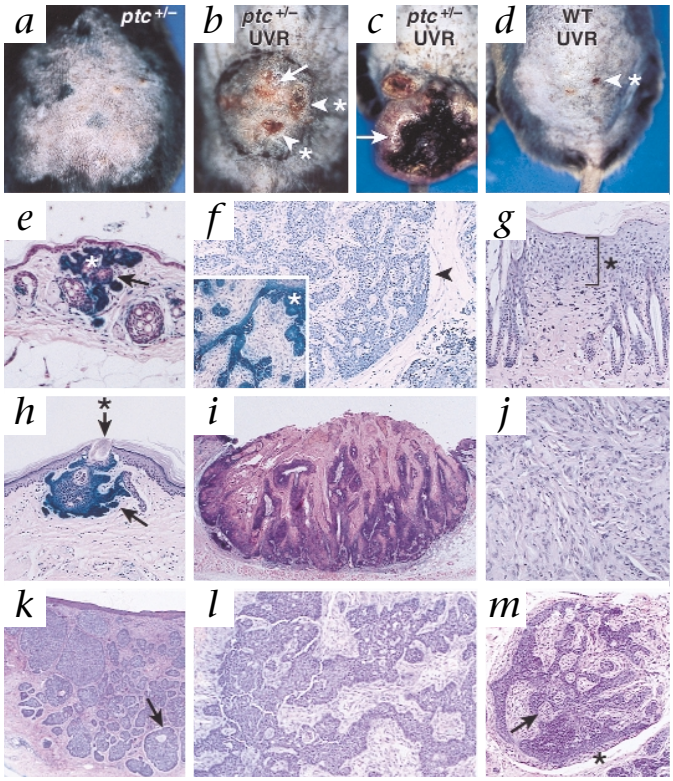

Fig. 1 Gross and histopathological findings. ***a***, ***e*** and ***h***, Untreated *Ptch*$^{+/-}$ mouse skin. ***b***, ***c***, ***f***, ***i***, ***j***, ***l*** and ***m***, UV-treated *Ptch*$^{+/-}$ mouse skin. ***d*** and ***g***, Wild-type (*Ptch*$^{+/+}$) UV-treated mice. ***k***, human BCC. *a*, Untreated, shaved *Ptch*$^{+/-}$ mice have no visible skin tumors on gross examination. *e*, Biopsy of grossly normal-appearing skin from a 17-month-old, untreated *Ptch*$^{+/-}$ mouse shows a small basaloid cell tumor that stains for β-gal (←), and within the tumor there are structures resembling hair follicles (*). Original magnification, ×10. *b* and *c*, Ptch$^{+/-}$ mice exposed to UV three times per week for 12 months have grossly visible BCCs (←) and keratoacanthomas (*➔). *f*, A large trichoblastoma from a *Ptch* $^{+/-}$ mouse treated with UV for 12 months has histologic features common to BCCs and trichoblastomas, including peripherally palisaded basaloid cells with enlarged nuclei, and few mitotic figures, but the tumor's cribiform tumor nest pattern and highly cellular stroma are features diagnostic of trichoblastoma. Clefting between mouse trichoblastoma tumor nests and stroma (➔) is often present. Original magnification, ×4. Inset, β-gal staining, indicative of hedgehog target gene activation, is confined to tumor nests of basaloid cells (*), and there is no staining in stromal cells. *i*, A *Ptch*$^{+/-}$ mouse treated with 12 months of UV exposure has a large keratoacanthoma. *j*, Fibrosarcomas often occur on UV-exposed *Ptch*$^{+/-}$ mice and are composed of spindle-shaped cells in a whorled pattern. *d* and *g*, A wild-type age-matched control littermate exposed to 12 months of UV has a small ulceration (*d*, *➔), which by biopsy (*g*) has histopathologic findings diagnostic of an *in situ* (intraepidermal) SCC (*). *h*, A trichoblastoma-like tumor (→) in the (UV-unexposed) paw pad of a UV-exposed *Ptch*$^{+/-}$ mouse. The stratum corneum overlying the BCC is thin (*) resulting in a paw 'pit'. *k* and *l*, The mouse BCC tumor in *l* has histologic features resembling those of nodular human BCCs (*k*), including irregular basaloid cell nests with peripheral cell palisading. Both mouse and human BCCs have clefting between the tumor nest and surrounding stroma (→) (*k*). *m*, In contrast, the mouse trichoblastoma-like tumors have a distinctive cribiform pattern and clefting between the tumor stroma and normal dermis (*) and have primitive hair follicle papillae structures that indent tumor nests (→).

not been reported to develop BCCs (refs. 14,15). Here, we report that *Ptch*$^{+/-}$ mice do develop a high incidence of BCC-like tumors (trichoblastomas and BCCs) in response to chronic UV exposure or to a single dose of ionizing radiation and thus represent the first mouse model, to our knowledge, of UV- and IR-induced BCC tumorigenesis.

Untreated *Ptch*$^{+/-}$ mice have microscopic skin tumors

Although the shaved skin of untreated *Ptch*$^{+/-}$ (exon 1/2) mice 3–17 months of age appeared grossly normal (Fig. 1*a*), skin biopsies showed that approximately 33% (30 of 91) had microscopically detectable proliferations resembling primordial hair follicle structures (Fig. 1*e*); none of 27 wild-type littermate control mice had skin tumors. Most of these small proliferations of basaloid cells (27 of 36) were in mice more than 9 months old (Table 1), indicating that mature *Ptch*$^{+/-}$ mice develop tumors that resemble human tumors of follicular origin even in the absence of experimental radiation exposure. Similarly, BCNS patients also develop multiple microscopic infundibulocystic BCCs (BCCs characterized by follicular differentiation) or proliferations of the follicular mantle on otherwise normal appearing and sometimes relatively UV-protected skin[16]. Paw biopsies showed distinctly demarcated stratum corneum defects or 'pits' with underlying BCC-like tumors (Fig. 1*h*), resembling the palmar pits of BCNS patients[17,18].

UV enhances BCC tumorigenesis in *Ptch* $^{+/-}$ mouse

We evaluated the effect of UV on mouse tumorigenesis by exposing *Ptch*$^{+/-}$ mice to UV at three times the minimal erythema dose (MED) (equivalent to a sunburn of moderate severity), three times per week, for up to 12 months. We found basaloid cell proliferations microscopically in irradiated areas of all UV-treated *Ptch*$^{+/-}$ mice (n = 26) ages 3–16 months (Table 1), and the tumor number and cross-sectional area increased considerably

Table 1 Skin tumor incidence size

	No treatment			Ultraviolet radiation			Cesium[a]		X-ray	
	Ptch$^{+/-}$ 3–8 months old	Ptch$^{+/-}$ > 9 months old	wild-type	Ptch$^{+/-}$ 3–8 months old	Ptch$^{+/-}$ > 9 months old	wild-type	Ptch$^{+/-}$	wild-type	Ptch$^{+/-}$	wild-type
Mice biopsied (n)	37	54	33	13	13	19	10	5	8	3
% with BCC	3%	40%	0%	100%	100%	0%	100%	0	100%	0
Average BCC number	1	0.5	0	7	9	0	12	0	17	0
Average BCC area (mm^2)	0.003	0.004	—	0.002	0.232	—	0.17	—	0.07	—
% with SCCs[b]	0%	0%	0%	0%	89% (8/9)	25%(4/16)	(%)	(%)	(%)	(%)
Average SCC number[b,c]	0	0	0	—	5.0*	2.8*	0	0	0	0
Average SCC area (mm^2)[b]	0	0	0	—	3.8	1.2	0	0	0	0

[a]Irradiation with 3 and 4 Gy cesium-137. [b]After 12 months of UV exposure. [c]Average of SCC-affected mice only. *, $P < 0.026$, one-tailed t-test.

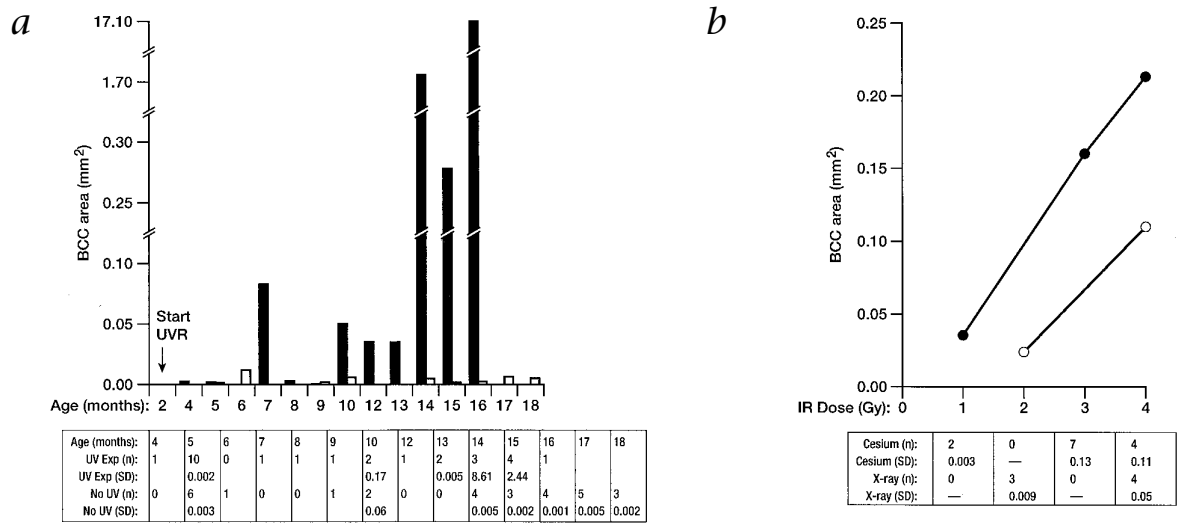

Fig. 2 BCC-like tumor average cross-sectional area increases with duration of UV exposure and dose of IR exposure. ***a***, Over time, UV exposure results in a substantial increase in the total cross-sectional area of BCCs in *Ptch*$^{+/-}$ mice (■) compared with that of untreated *Ptch*$^{+/-}$ age-matched control mice (□); $P < 0.03$; one-tailed Student's *t*-test. ***b***, IR exposure with either cesium-137 (●) or X-ray (○) results in a dose-dependent increase in the total cross-sectional area of trichoblastoma: 1–4 Gy cesium-137, $P < 0.0065$; 2–4 Gy X-ray, $P < 0.0163$; both one-tailed Student's *t*-test.

with increased duration of UV exposure (2–8 months, 0.0004–0.08 mm^2; 10–16 months, 0.03–17.1 mm^2) (Fig. 2*a*). Basaloid cell tumors in unirradiated skin of these mice were, on average, smaller in diameter by at least 400%. There were no BCC-like tumors in skin biopsies from UV-exposed wild-type littermate control mice ($n = 19$). There was no difference in skin thickness or number of apoptotic keratinocytes in wild-type compared with *Ptch*$^{+/-}$ mice 48–72 hours after exposure to a single 3 MED dose of UV.

Grossly visible tumors were first apparent in irradiated skin after 4 months of UV exposure in *Ptch*$^{+/-}$ mice, but only after 11 months of UV exposure in the wild-type control mice; the latter had only SCC-type tumors. The tumors in the *Ptch*$^{+/-}$ mice grew rapidly, doubling in size approximately every 4 weeks. By 11 months of UV exposure, 86% (19 of 22) of the irradiated *Ptch*$^{+/-}$ mice, compared with 16% (4 of 24) of the control wild-type littermates, had developed visible cutaneous tumors (Fig. 1*b–d*). The visible tumors in the *Ptch*$^{+/-}$ mice were 15-fold larger (average, 175 mm^3 compared with 12 mm^3) and twice as numerous (average, 3.6 compared with 1.8 tumors per affected mouse). Of the visible tumors biopsied ($n = 21$) in the *Ptch*$^{+/-}$ mice, approximately 20% were BCCs or trichoblastomas (tumors with follicular differentiation that share many histologic features with BCCs), 30% were SCCs or keratoacanthomas (SCC-like tumors) and 50% were fibrosarcomas or fibromas. BCC and trichoblastoma-like tumors were grossly translucent ulcerated papules identical in appearance to human BCCs (Fig. 1*b*) or were violaceous superficial dermal nodules (Fig. 1*c*). Fibrosarcomas were firm, pink, generally pedunculated nodules, some as large as 20 mm^3; and keratoacanthomas were papules with central craters filled with hard keratinous material (Fig. 1*i*). Wild-type control littermates exposed to UV developed smaller ulcerated papules (Fig. 1*d*) that by histology were invasive or *in situ* SCCs (Fig. 1*g*). Wild-type mice did not develop BCC-like tumors or fibrosarcomas.

Ionizing radiation enhances BCC tumorigenesis in *Ptch*$^{+/-}$ mice

BCCs occur with greater incidence in portals of radiotherapy, both in the general population and especially in BCNS patients, indicating that ionizing radiation (IR) may be another common *PTCH* mutagen[19,20]. Therefore, we also evaluated the effect of IR exposure on BCC tumorigenesis in *Ptch*$^{+/-}$ mice. All *Ptch*$^{+/-}$ mice treated at 2 months of age with a single dose of X-ray or cesium radiation had microscopically detectable trichoblastoma-like tumors in biopsies obtained 12 months after treatment (Fig. 2*a* and *b*). The IR increased trichoblastoma-like tumor numbers and size in a dose-dependent manner (Fig. 2*b*). Trichoblastoma-like tumors induced by cesium-137 and X-ray radiation were grossly and histologically indistinguishable from UV-induced trichoblastoma-like tumors. In contrast to UV-exposed *Ptch*$^{+/-}$ mice, IR-exposed mice did not develop fibrosarcomas or SCCs. Wild-type control littermates ($n = 12$) treated with the same dose of either cesium or X-ray radiation had no detectable skin abnormalities.

Histology resembles human trichoblastomas and BCCs

All biopsies from *Ptch*$^{+/-}$ mouse skin exposed to 2–7 months of UV had multiple, microscopic, dermally invasive 'buds' of basaloid cells emerging from either the interfollicular epidermis or the follicular infundibulum, and the origin and appearance of these 'buds' were similar to those of superficial human BCCs. Mice exposed to more than 7 months of UV (9 months of age) had tumors with histology that most closely resembled that of a human trichoblastoma or BCC, and these were on average 100 times larger than the early 'buds' (0.002 mm^2 compared with 0.23 mm^2). After 12 months of chronic UV exposure, all *Ptch*$^{+/-}$ mice had tumors with histologic features of human BCCs. Of these tumors, 44% were best classified as superficial, mostly interfollicular basaloid proliferations, 13% (4 of 30) had histologic features diagnostic of nodular or infiltrating human BCCs (Fig. 1*l*) and 43% (13 of 30) had features of trichoblastoma (Fig. 1*m*). Like human BCCs, mouse trichoblastoma and BCC-like tumors are composed of nests of basaloid cells with large nuclei, scant cytoplasm and few mitotic figures. Some mouse BCC and trichoblastoma tumor nests have peripheral palisading and small

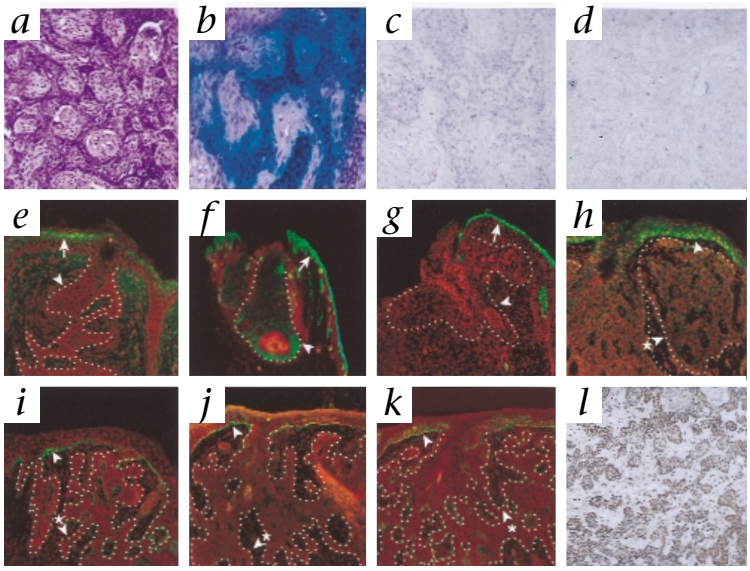

Fig. 3 *In situ* detection of hedgehog target genes and immunohistology of *Ptch*$^{+/-}$ mouse BCC differentiation markers, hemidesmosomal proteins and Bcl2 protein. ***a–d***, A trichoblastoma-like tumor induced by cesium radiation stained with hematoxylin and eosin (*a*) demonstrates high levels of *Ptch* promoter activation and thus *lacZ* expression (*b*), low levels of *Gli* mRNA within tumor nests using an antisense probe (*c*) and no staining with a *Gli* sense probe (*d*). ***e–g***, *Ptch*$^{+/-}$ mouse BCC-like and trichoblastoma-like tumors (outlined with ···) and overlying epidermal cells are counterstained (red) with 7-AAD. Like human BCCs, the *Ptch*$^{+/-}$ mouse tumors do not stain for the differentiation markers keratin 10 (*e*, ➔) or loricrin (*g*, ➔) but do stain strongly (green) for the basal cell marker keratin 14 (*f*, ➔). In contrast, the overlying epidermis (→) is strongly positive for keratin 10 (*e*), keratin 14 (*f*) and loricrin (*g*). ***h–k***, Mouse epidermis stains strongly along the basement membrane (➔) for BP180 (*h*), the γ2 subunit of LAM5 (*i*), and β4 (*j*) and α6 integrins (*k*), but BCC-like tumors (outlined with····) have diminished staining for α6 integrin (*k*) and substantially diminished immunoreactivity for BP180 (*h*), LAM5 (*i*), and β4 integrin (*j*). ***l***, Mouse BCCs stain with antibody against mouse Bcl2 diffusely throughout tumor nests, which is typical of human BCCs.

cysts lined by cornified cells reminiscent of hair follicle structures (Fig. 1*e*). Clefts between tumor nests and surrounding connective-tissue stroma, an important diagnostic hallmark of human BCCs (Fig. 1*k*), were also present in some mouse trichoblastomas and in BCC-like tumors (Fig. 1*f*). Mirroring the characteristic histopathologic features of human BCCs, even the largest mouse BCC-like tumors (maximum cross-sectional area of 452 mm^2) were well-circumscribed, symmetrical and locally destructive, but they did not invade muscle or bone and did not metastasize. The mouse trichoblastoma-like tumors had the features described above, but, in contrast to the mouse BCC-like tumors, were well-circumscribed, had abundant collagenous stroma with clefts separating tumor stroma from normal dermis, had cribiform or reticulated tumor nests and had focal accumulations of dermal fibroblasts resembling hair papillae that abutted on or 'enveloped' the tumor nests (Fig. 1*m*).

LacZ reporter and *Gli1* expressed in mouse BCCs

High levels of *PTCH* mRNA and *Gli1* mRNA are detected in almost all human BCCs, and this is consistent with the present model of inhibition of transcription of *PTCH* as well as of other hedgehog target genes by PTCH protein. Therefore, mouse BCC-like tumor cells with loss of functional Ptch protein would be predicted to have de-repressed transcription of the *lacZ* gene inserted at the inactivated *Ptch* locus and, consequently, high levels of β-galactosidase (β-gal). Indeed, we did detect high levels of β-gal in all *Ptch*$^{+/-}$ mouse BCC and trichoblastoma-like tumors assessed, including two tumors with confirmed complete *Ptch* gene inactivation. Small (0.001 mm^2) and large (greater than 2.0 mm^2) BCC and trichoblastoma-like tumors had β-gal staining throughout the tumor (Fig. 1*f*, inset). Normal epidermis, exposed or unexposed to UV, did not stain for β-gal. All 12 BCC-like and trichoblastoma-like tumors (sizes, 0.0025–1.3 mm^2) examined by *in situ* analysis had detectable *Gli* mRNA (Fig. 3*c* and *d*). In contrast, two SCCs did not have detectable *Gli* mRNA, and no SCCs stained for β-gal. Most fibrosarcomas (Fig. 1*j*) stained positive for β-gal, and positive staining for vimentin and negative staining for keratin confirmed their fibroblastic derivation. These results indicate that activation of hedgehog targets such as *Ptch* occurs in BCC and trichoblastoma-like tumors and in some fibrosarcomas but not in SCCs. Furthermore, cells in the follicular bulge region of UV- and IR-treated and untreated mice often had high levels of β-gal, indicating that hedgehog target gene activation occurs in the bulge region. The follicular bulge is stem cell-rich, and it may be the primary site of origin of both BCC and other skin cancer cells[21].

Mouse and human BCCs have similar immunohistology

Mouse BCC and trichoblastoma-like tumors (n = 3) showed patterns of protein expression similar to those of human BCCs: the presence of a basal cell marker (keratin 14) (Fig. 3*f*), the absence of suprabasalar epidermal differentiation markers (keratin 10 and loricrin) (Fig. 3*e* and *g*), reduced immunoreactivity of hemidesmosomal components (BP180, β4 integrin, a6 integrin and the ϒ2 chain of LAM5)(Fig. 3*h–k*), and staining for Bcl2 antigen diffusely within tumor nests (Fig. 3*l*) (refs. 22,23,24,25).

Mouse tumors have *Ptch* loss of heterozygosity

Because as many as 60% of human sporadic and BCNS-related BCCs have loss of one *PTCH* allele[7,26], and *PTCH* mutations have also been identified in some human trichoepitheliomas (a subtype of trichoblastoma), we screened mouse BCC and trichoblastoma-like tumors for loss of wild-type *Ptch*. We detected loss of the *Ptch* wild-type allele and retention of the mutant allele in both mouse BCC and trichoblastoma-like tumors (two of five in UV-exposed mice; two of two in cesium-137 irradiated mice) and in fibrosarcomas (two of four in UV-exposed mice) but not (consistent with their lack of β-gal staining) in six biopsies of UV-exposed skin adjacent to or overlying these tumors, two SCCs or three fibromas. Because mutations in the *p53* gene have been identified in 44–61% of human BCCs (refs. 27 and 28), we screened UV-exposed *Ptch*$^{+/-}$ mouse skin BCCs and trichoblastoma-like tumors for mutations in exons 5–8 of *p53*. We identified *p53* mutations in two of five of the mouse trichoblastoma and BCC-like tumors, one of seven fibrosarcomas, and one of two mouse SCCs from UV-exposed *Ptch*$^{+/-}$ mice (Table 2). Four of the identified mutations were of the UV 'signature type' (C→T or CC→TT) and commonly occurred at or adjacent to mouse *p53* mutation 'hot spots'. The p53 mutations did not correlate with tumor aggressiveness. We detected no *p53* abnormalities in unirradiated mouse tail (n = 3), UV-exposed skin adjacent to tumors (n = 5), one BCC-like tumor from a cesium irradiated *Ptch*$^{+/-}$ mouse, one SCC from a wild-type mouse and two spontaneous rhabdomyosarcomas.

Mouse trichoblastoma maintained in culture

To confirm the neoplastic nature of the mouse BCC-like tumors, we attempted to culture three mouse trichoblastoma-like tumors. We passaged cells from one mouse trichoblastoma-like tumor with both loss of the wild-type *Ptch* allele and two distinct *p53* mutations twice, and have cultured these successfully, for 10 months so far. These cells have loss of the wild-type *Ptch* allele and retain both of the *p53* mutations identified in the original tumor, thus confirming their derivation from the tumor rather than from normal keratinocytes. These cells proliferate slowly, as do cultured human BCC cells[29]. In contrast to the original mouse tumor, cultured trichoblastoma cells fail to express β-gal. Attempts to engraft cultured cells onto nude mice have failed.

Ptch$^{+/-}$ mice have a higher incidence of SCCs

Most wild-type mice biopsied after 11 months of UV exposure (13 of 16) had at least one microscopically detectable skin cancer, most commonly SCC *in situ* (65%). Only 25% (4 of 16) of wild-type control mice biopsied after 12 months of UV exposure had invasive SCCs, and the ratio of *in situ* to invasive SCCs was 3:1. In contrast, invasive SCCs or keratoacanthomas occurred in 57% (8 of 14) of *Ptch*$^{+/-}$ mice receiving 11 to 12 months of UV exposure, and the ratio of *in situ* to invasive SCCs or keratoacanthomas was 1.5:1. Furthermore, the SCCs in *Ptch*$^{+/-}$ mice were on average threefold larger than those of the wild-type mice (3.8 mm^2 compared with 1.2 mm^2) (Table 1). Therefore, *Ptch*$^{+/-}$ mice more commonly develop invasive SCCs or keratoacanthomas ($P < 0.026$, one-tailed *t*-test), and these tumors are considerably larger than those in their wild-type control littermates.

Ptch$^{+/-}$ mice do not have impaired immune function

Because host immune function may substantially influence susceptibility to skin photocarcinogenesis[30], we compared mouse ear swelling test responses after application of dinitrochlorobenzene, as a measure of delayed-type hypersensitivity in 3-month-old *Ptch*$^{+/-}$ and wild-type mice exposed to UV three times weekly for 1–1.5 months. In addition, we did mouse ear swelling tests on a group of *Ptch*$^{+/-}$ mice and wild-type mice 15 months of age that had been exposed to either a single dose of cesium-137 or of X-ray radiation at 2 months of age. There was no statistically significant difference in delayed type hypersensitivity response between *Ptch*$^{+/-}$ mice and wild-type mice in the UV- and IR-treated groups. Furthermore, in IR-treated *Ptch*$^{+/-}$ mice, there was no correlation between tumor volume and mouse ear swelling test response. The equivalent delayed- type hypersensitivity responses in wild-type and *Ptch*$^{+/-}$ mice and lack of variation with tumor number indicate that increased tumorigenesis in *Ptch*$^{+/-}$ mice is unrelated to differences in immune surveillance.

Discussion

The *Ptch*$^{+/-}$ mouse represents a new model of spontaneous and UV/IR-enhanced BCC and trichoblastoma tumorigenesis. Treatment of a variety of inbred mouse (*Ptch*$^{+/+}$) strains with UV, IR or topical chemical carcinogens readily induces cutaneous papillomas and SCCs, but these treatments induce BCCs only rarely[11,31]. Although rats seem to develop BCCs with application of carcinogens or exposure to IR, mice do not show equal susceptibility. Background genes may confer the relative resistance of the mouse species to BCCs and the *Ptch*$^{+/-}$ genetic abnormality may overwhelm these protective mechanisms. Our mouse model of BCCs is based closely on the genetics of the human tumor, and allows reproducible and frequent production of BCC-like and trichoblastoma-like tumors. The irradiated *Ptch*$^{+/-}$ mouse confirms a direct causal relationship between exposure to UV and IR and BCC tumorigenesis, thus establishing the importance of protection from UV and IR in humans to prevent these cancers. The *Ptch*$^{+/-}$ mouse is a representative model of the human BCNS patient (*PTCH*$^{+/-}$) in that both the mice and humans develop medulloblastomas and rhabdomyosarcomas, develop small basaloid cell tumors with aging on skin protected from UV, and develop larger and more numerous BCC-like tumors in UV- and IR-exposed skin. Therefore, the *Ptch*$^{+/-}$ mouse provides an ideal *in vivo* model to test corrective gene therapy, chemoprevention, or chemotherapy in treating BCC tumors. Furthermore, the observation that *Ptch*$^{+/-}$ mice are also susceptible to trichoblastomas is consistent with the observation that some human trichoepitheliomas, a sub-type of trichoblastoma, have *PTCH* gene mutations.

The mouse BCC and trichoblastoma-like tumors are identical to human BCCs in their induction of the hedgehog target genes (as indicated by *Ptch* promoter activation and *Gli* mRNA detection), diminished hemidesmosomal protein expression, and frequent wild-type *Ptch* gene deletion. The deletion of the wild-type *Ptch* gene in almost all cells of some BCC and trichoblastoma-like tumors from *Ptch*$^{+/-}$ mice exposed to UV or IR confirms that the *Ptch* gene itself is an important target for radiation-induced mutagenesis and that *Ptch*$^{-/-}$ cells may undergo clonal expansion. Moreover, the consistent staining of all early mouse BCC and trichoblastoma-like tumors for β-gal and absence of staining in adjacent histologically normal UV-exposed skin indicate that hedgehog signaling pathway dysregulation and pathway target gene activation is the essential event in initiation of BCC tumorigenesis. These findings are consistent with animal models in which overexpression of *Shh*, *smo*^{mut} or *Gli1* is tumorigenic.

Involvement of abnormalities of the *p53* gene in BCC tumorigenesis was indicated by the occurrence of *p53* gene mutations in 40% (two of five) of BCC and trichoblastoma-like tumors from UV-exposed mice (Table 2), which is consistent with the observed incidence (44 to 61%) of *p53* mutations in human BCCs (refs. 27,28). These *p53* mutations occurred at reported mutation 'hot spots', and several were UV 'signature-type' mutations (C→T or CC→TT). Attempts to correlate loss of heterozygosity at the human *PTCH* locus and mutations in *p53* have shown no statistically significant correlation between these two genetic defects and histologic type[28]. Although the occurrence of *p53* mutations and high levels of staining for Bcl2 in both human and mouse BCCs indicate involvement of cell growth and apoptosis regulatory genes in BCC tumorigenesis, there is no known

Table 2 p53 mutations in tumors of UV-treated Ptch$^{+/-}$ mice

Tumor	Histology	Exposure	Exon	Codon	Mutation	Result
1	BCC	UV	5	149	CCA→CTA	Pro→Leu
				176	CAT→TAT	His→Tyr
2	BCC	UV	8	275	CCT→GCT	Pro→Ala
3	SCC	UV	5	137	ACG→ATG	Thr→Met
4	Fibrosarcoma	UV	8	274/275	TGCCCT→TGTTCT	Pro→Ser
			8	266	AGC→GGC	Ser→Gly
			8	267	TTT→TCT	Phe→Ser

UV, ultraviolet radiation.

direct interaction between the effects of hedgehog signaling pathway dysregulation and those of *p53* gene mutation.

The size and frequency of SCCs also were increased in *Ptch*$^{+/-}$ mice treated with UV, compared with those in wild-type control mice. It seems that the mechanism by which *Ptch* hemizygosity predisposes mice to SCCs is not induction of hedgehog target gene either chronically or acutely, as β-gal staining was negative in the *Ptch*$^{+/-}$ mice in both SCCs and in normal UV-exposed skin. Similarly, in the small number of SCCs studied, there was no wild-type allele inactivation (two of two SCCs retained heterozygosity). Genetic and epidemiologic evidence, including studies of BCNS patients, have not established a relationship between *PTCH* hemizygosity and SCC predisposition in humans. However, our results in mice and reports of loss of heterozygosity at 9q (the *PTCH* locus) in a minority of human SCCs (3 of 14; ref. 32) indicate a potential role for *PTCH* in the regulation of SCC tumorigenesis. Our preliminary studies of acute response to UV exposure and delayed type hypersensitivity response have failed to elucidate host factors in *Ptch*$^{+/-}$ mice that could predispose to SCC. Further studies will be required to evaluate the role of *PTCH* inactivation in human SCCs.

Methods

Mice. The *Ptch*$^{+/-}$ mice studied were C57BL/6 and DBA/2J F1 hybrids, and were heterozygous for a deletion of exons 1 and 2 and insertion of the *lacZ* and *neo* genes. *Ptch*$^{+/-}$ mice were genotyped using PCR primers specific to the *neo* insert and wild-type regions as described[14]. The mice ate Purina 5008 laboratory chow and drank water *ad libitum*, were housed in plastic cages with metal lids in animal quarters lacking natural light and with 50% humidity and ambient temperature of 70 to 74 °F, and were exposed daily to 12 h of white light from 34-watt fluorescent bulbs.

Exposure of mice to UV and IR. UV was delivered three times per week at 3 MED (177 mJ/cm^2 ultraviolet B) using an air-cooled Hanovia (Aero-Kromayer, Newark, New Jersey) hot quartz contact lamp, which emits 229 mJ/cm^2 per second of ultraviolet C, 59 mJ/cm^2 per second of ultraviolet B and 221 mJ/cm^2 per second of ultraviolet A at a distance of 1.9 cm. The back hair of the mice was clipped with barber shears before the initial UV exposure and at 3- to 4-week intervals thereafter. An area of exposed skin 2.5 cm in diameter on the mid-back at the level of the hind limbs was irradiated at a distance of 1.9 cm for 3 s three times per week starting at the age of 2 months and for a total of 12 months[33,34]. The radiation energy was measured with a Hanovia Ultraviolet meter (model AV-97; Aero-Kromayer, Newark, New Jersey). UV-exposed skin became erythematous and scaly, but no other UV-associated morbidity or mortality was noted. Of all the UV-exposed *Ptch*$^{+/-}$ mice, 12% (4 of 33) developed medulloblastomas and 9% (3 of 33) developed rhabdomyosarcomas. There was no substantial difference in the incidence of these extracutaneous tumors in UV-exposed and untreated *Ptch*$^{+/-}$ mice.

At 2 months of age, *Ptch*$^{+/-}$ mice and wild-type control littermates were anesthetized with ketamine and xylazine and were treated with unfiltered X-ray (250 kV) at 15 mamp, half-value layer, (HVL) 1.8 mm Cu, for a total dose of either 2 or 4 Gy at the target skin distance of 38.5 cm, using the Westinghouse Quadrocondex (dose rate of 2.54 Gy/min) or gamma radiation delivered by the Best Industries (Springfield, Virginia) cesium-137 radiation device (half-value layer, 0.60 cm Pb; dose rate, 0.94 Gy/min) with total radiation doses of 1, 3 or 4 Gy. One of twenty-four mice died 1 d after IR treatment; one of nine X-ray-exposed *Ptch*$^{+/-}$ mice developed a medulloblastoma and two *Ptch*$^{+/-}$ mice (one cesium- and one X-ray-exposed) developed large rhabdomyosarcomas of the hind limb. All other mice survived the subsequent year, and no acute morbidity, including dermatitis, was noted.

Tumor sampling and quantification. A circular area of caudal back skin 2.5 cm in diameter (corresponding to the site of UV treatment in UV-exposed mice) was excised from anesthetized mice, and was divided into five slivers 0.5 cm in thickness, fixed in 10% buffered formalin for routine staining with hematoxylin and eosin or processed for staining with β-gal. Tumor area was determined by measuring the two-dimensional cross-sectional size of all BCC-like tumors found in the five skin slivers, thereby maintaining equal random sampling among all study groups. Here, total BCC area is the sum of the cross-sectional areas of all BCC-like tumors observed in the five sections taken from the 2.5-cm sample area. Statistical analysis used a one-tailed Student's *t*-test for data sets of unequal variance. In 70% of tumor-bearing mice, gross examination and biopsies to ascertain tumor metastasis were obtained from local and distant lymph nodes, liver, lungs and spleen.

Immunohistology. Skin samples of mouse BCC or trichoblastoma-like tumors were embedded in OCT and sections 8 μm in thickness were cut, air-dried, and fixed in 4% paraformaldehyde. Sections were then washed with PBS and blocked with 10% normal goat serum with 0.1% Triton X-100. Tissue was incubated with antibodies for 2 h at room temperature, washed with PBS, and incubated for 1 h with a corresponding FITC-labeled secondary antibody and a 7-AAD (1:100 dilution) counterstain. Alternatively, samples incubated with antibodies against Bcl2 and vimentin were subsequently incubated with biotinylated secondary antibodies followed by staining with horseradish peroxidase and DAB. Sections were viewed using confocal or light microscopy. Antibodies used included control rabbit immunoglobulin (1:250 dilution) and mouse antibody against K10 (1:100 dilution)(both from Dako, Carpinteria, California), rabbit antibodies against K14 (1:500 dilution) and loricrin (1:500 dilution)(both from BAbCo, Maspeth, New York), rabbit antibody against BP180 (1:1,000 dilution; a gift from Z. Liu), rabbit antibody against lam 5 (1:100 dilution; a gift from D. Aberdam), rat α6 integrin (1:100 dilution; a gift from P. Marinkovich), rat antibody against β4 (1:100 dilution; RDI, Flanders, New Jersey)[35,36,37], goat antibody against vimentin (1:40 dilution; Sigma), and polyclonal rabbit antibody against mouse Bcl2 (1:800 dilution; PharMingen, San Diego, California)[38].

β-gal stain. *LacZ*-encoded bacterial β-galactosidase was detected by incubation of glutaraldehyde and formalin fixed tissue with X-gal and iron buffer solution (Boehringer) for 48 h.

***In situ* analysis.** Twelve tumors ranging in size from 0.0025 to 1.3 mm^2 were examined. *In situ* hybridization studies used a standard protocol and paraffin-embedded mouse tumor tissue, with antisense and sense control probes. The *Gli1* template was a mouse *Gli1* partial cDNA provided by A.A. Joyner (New York University).

Assessment of *Ptch* loss of heterozygosity. Freshly excised mouse BCC-like tumors (n = 5), SCCs (n = 2) and fibrosarcomas (n = 7) were dissected from overlying epidermis and dermal stroma. DNA was extracted, and PCR primers specific to the wild-type exon 1 site and *neo* inserts were used as described[14].

p53 mutation detection. DNA from BCC-like tumors (n = 5), fibrosarcomas (n = 7), SCCs (n = 2) and normal-appearing skin (n = 4) from UV-exposed sites of *Ptch*$^{+/-}$ mice, one BCC-like tumor from a cesium-exposed *Ptch*$^{+/-}$ mouse and one SCC from a wild-type UV-exposed mouse were screened for p53 mutations using single-strand conformational polymorphism analysis using primers for exons 5, 6, 7 and 8 (ref. 39). Controls were unirradiated tail DNA (n = 3) and two spontaneous rhabdomyosarcomas. Tumor DNA exons with detectable single-strand conformational polymorphism abnormalities were cloned into plasmid vector pCR2.1 and sequenced using the ABI Prism sequencer (Foster City, California).

BCC tumor cell culture. BCC-like tumors were grossly dissected from epidermis and normal dermis, placed in DMEM media supplemented with 10% FCS, penicillin/streptomycin and fungizone, and incubated 12 h at 4 °C in media containing 0.25% trypsin. Earl's BSS medium with 10% FCS was added, and cells were centrifuged at 1,000 rpm for 5 min. The pellet was resuspended in 5 ml of 154CF media (Cascade Biologics, Portland, Oregon) supplemented with gentamicin, and was then plated and incubated at 37 °C in an atmosphere of 7% CO_2.

Immune response to topical dinitrochlorobenzene. *Ptch*$^{+/-}$ mice and wild-type littermates were sensitized by application to their shaved abdomens of 50 μl of 4% dinitrochlorobenzene (Sigma) in a vehicle of ace-

tone and olive oil; 7 d after sensitization, immune response was elicited by application of 2% dinitrochlorobenzene or vehicle alone (25 μl) to the pinnae as described[40]. Ear thickness measurements were obtained with a digital micrometer (Mitutoyo, Japan) before elicitation and 24 and 48 h after elicitation in *Ptch*$^{+/-}$ mice not exposed to UV or IR (n = 12), treated with UV for 1–1.5 months (n = 14) or treated 12 months before with a single dose of cesium or X-ray irradiation (n = 12), and in wild-type littermate control mice treated similarly (n = 7, n = 11, or n = 9).

Acknowledgments

We thank L. Goodrich for providing the Ptch$^{+/-}$ *mouse, M. Weinstein and S. Pennypacker for technical assistance, and R. Szabo for his critical input. This work was supported by grants from the National Institutes of Health (AR39959, AR4311 and CA81888) (E.H.E.), fellowships from the Dermatology Foundation (M.A.), and donations from P. Hughes and from the Michael J. Rainen Family Foundation. M.P.S. is an Investigator of the Howard Hughes Medical Institute.*

RECEIVED 20 AUGUST; ACCEPTED 10 SEPTEMBER

1. Miller, D.L. & Weinstock, M.A. Non-melanoma skin cancer in the United States: incidence. *J. Am. Acad. Dermatol.* **30**, 774–778 (1994).
2. Hahn, H. *et al.* Mutations of the human homolog of Drosophila *patched* in the nevoid basal cell carcinoma syndrome. *Cell* **85**, 841–851 (1996).
3. Johnson, R.L. *et al.* Human homolog of patched, a candidate gene for the basal cell nevus syndrome. *Science* **272**, 1668–1671 (1996).
4. Vorechovsky, I., Unden, A.B., Sandstedt B., Toftgard, R. & Stahle-Backdahl, M. Trichoepitheliomas contain somatic mutations in the overexpressed PTCH gene: support for a gatekeeper mechanism in skin tumorigenesis. *Cancer Res.* **57**, 4677–4681 (1997).
5. Raffel, C. *et al.* Sporadic medulloblastomas contain PTCH mutations. *Cancer Res.* **57**, 842–845 (1997).
6. Xie, J. *et al.* Mutations of the PATCHED gene in several types of sporadic extracutaneous tumors. *Cancer Res* **57**, 2369–2372, (1997).
7. Gailani, M.R. *et al.* The role of the human homologue of *Drosophila patched* in sporadic basal cell carcinomas. *Nature Genet.* **14**, 78–81 (1996).
8. Kallassy, M. *et al.* Patched (ptch)-associated preferential expression of smoothened (smoh) in human basal cell carcinoma of the skin. *Cancer Res.* **57**, 4731–4735 (1997).
9. Dahmane, N., Lee, J., Robins, P., Heller, P. & Ruiz i Altaba, A. Activation of the transcription factor Gli1 and the sonic hedgehog signalling pathway in skin tumours. *Nature* **389**, 876–880 (1997).
10. Green, J., Leigh, I.M., Poulsom R., Quinn, A.G. Basal cell carcinoma development is associated with induction of the expression of the transcription factor Gli-1. *Br. J. Dermatol.* **139**, 911–915 (1998).
11. Bogovski, P. in *Tumours of the Mouse. Pathology of Tumours in Laboratory Animals* Vol. *2* (eds. Turusov, V.S. & Mohr, U.) 11–12 (International Agency for Research on Cancer, Lyon, 1994).
12. Oro, A.E. *et al.* Basal cell carcinomas in mice overexpressing sonic hedgehog. *Science* **276**, 817–821 (1997).
13. Xie, J. *et al.* Activating Smoothened mutations in sporadic basal-cell carcinoma. *Nature* **391**, 90–92 (1998).
14. Goodrich, L.V., Milenkovic, L., Higgins, K.M., & Scott, M.P. Altered neural cell fates and medulloblastoma in mouse patched mutants. *Science* 277, 1109–1113 (1997).
15. Hahn, H. *et al.* Rhabdomyosarcomas and radiation hypersensitivity in a mouse model of Gorlin syndrome. *Nature Med.* **4**, 619–622 (1998).
16. Walsh, N., Ackerman, A.B. Infundibulocystic basal cell carcinoma: a newly described variant. *Mod. Path.* **3**, 599–608 (1990).
17. Gorlin, R.J. Nevoid basal cell carcinoma syndrome. *Medicine* **66**, 98–109 (1987).
18. Hashimoto, K., Howell, J.B., Yamanishi, Y., Holubar, K. & Bernhard, R. Electron microscopic studies of palmar and plantar pits of nevoid basal cell epithelioma. *J. Invest. Dermatol.* **59**, 380–393 (1972).
19. Karagas, M.R. *et al.* Risk of basal cell and squamous cell skin cancers after ionizing radiation therapy. *J. Natl. Cancer Inst.* **88**, 1848–1852 (1996).
20. O'Malley, S. *et al.* Multiple neoplasms following craniospinal irradiation for medulloblastoma in a patient with nevoid basal cell carcinoma syndrome. *J. Neurosurg.* **86**, 286–288 (1997).
21. Miller, S.J., Tung-Tien, S. & Lavker, R.M. Hair follicles, stem cells, and skin cancer. *J. Invest. Dermatol.* **100**, 288S–294S (1993).
22. Markey, A.C., Lane, E.B., MacDonald, D.M. & Leigh, I.M. Keratin expression in basal cell carcinomas. *Br. J. Dermatol.* **126**, 154–160 (1992).
23. Fairley, J.A., Heintz, P.W., Neuburg, M., Diaz, L.A. & Giudice, G.J. Expression pattern of the bullous pemphigoid-180 antigen in normal and neoplastic epithelia. *Br. J. Dermatol.* **133**, 385–391 (1995).
24. Bahadoran, P. *et al.* Altered expression of the hemidesmosome-anchoring filament complex proteins in basal cell carcinoma: possible role in the origin of peritumoral lacunae. *Br. J. Dermatol.* **136**, 35–42 (1997).
25. Smoller, B.R., Van de Rijn, M., Lebrun, D. & Warnke, R.A. Bcl-2 expression reliably distinguishes trichoepitheliomas from basal cell carcinomas. *Br. J. Dermatol.* **131**, 28–31 (1994).
26. Bonifas, J.M., Bare, J.W., Kerschmann, R.L., Master, S.P. & Epstein, E.H. Jr. Parental origin of chromosome 9q22.3-q31 lost in basal cell carcinomas from basal cell nevus syndrome patients. *Hum. Mol. Genet.* **3**, 447–448 (1994).
27. Van der Riet, P. *et al.* Progression of basal cell carcinoma through loss of chromosome 9 and inactivation of a single p53 allele. *Cancer Res.* **54**, 25–27 (1994).
28. Gailani, M.R. *et al.* Relationship between sunlight exposure and a key genetic alteration in basal cell carcinoma. *J. Natl. Cancer Inst.* **88**, 349–354 (1996).
29. Grando, S.A. *et al.* Nodular basal cell carcinoma *in vivo* vs. *in vitro*. *Arch. Dermatol.* **132**, 1185–1193 (1996).
30. Nishigori, C., Yarosh, D.B., Danawho, C. & Kripke, M.L. The immune system in ultraviolet carcinogenesis. *J. Invest. Dermatol. Symp. Proc.* **1**, 143–146 (1996).
31. Della Porta, G., Terracini, B., Dammert, K. & Shubik, P. Histopathology of tumors induced in mice treated with polyoxyethylene sorbitan monostearate. *J. Natl. Cancer Inst.* **25**, 573–605 (1960).
32. Quinn, A.G., Campbell, C., Healy, E. & Rees, J.L. Chromosome 9 allele loss occurs in both basal and squamous cell carcinomas of the skin. *J. Invest. Dermatol.* **102**, 300–303 (1994).
33. Epstein, J.H. Comparison of the carcinogenic and cocarcinogenic effects of ultraviolet light on hairless mice. *J. Natl. Cancer Inst.* **34**, 741–745 (1965).
34. Epstein, J.H. in *Models in Dermatology* Vol 2 (eds. Maibach, H. & Lowe, N.J.) 303–312 (Karger, Basel, 1985).
35. Guo, L., Yu, Q.-C. & Fuchs, E. Targeting expression of keratinocyte growth factor to keratinocytes elicits striking changes in epithelial differentiation in transgenic mice. *EMBO J.* **12**, 973–986 (1993).
36. Liu, Z. *et al.* A passive transfer model of the organ-specific autoimmune disease, bullous pemphigoid, using antibodies generated against the hemidesmosomal antigen, BP180. *J. Clin. Invest.* **92**, 2480–2488 (1993).
37. Aberdam, D. *et al.* Developmental expression of nicein adhesion protein (laminin 5) subunits suggests multiple morphogenic roles. *Cell Adhes. and Commun.* **2**, 115–129 (1994).
38. Krajewski, S. *et al.* Immunohistochemical determination of in vivo distribution of bax, a dominant inhibitor of bcl-2. *Am. J. Path.* **145**, 1323–1336 (1994).
39. Kress, S. *et al.* Carcinogen-specific mutational pattern in the *p53* gene in ultraviolet B radiation-induced squamous cell carcinomas of mouse skin. *Cancer Res.* **52**, 6400–6403 (1992).
40. Garrigue, J.L. *et al.* Optimization of the mouse ear swelling test for *in vivo* and *in vitro* studies of weak contact sensitizers. *Contact Dermatitis* **30**, 231–237 (1994).